Br. J. Pharmacol. (1994), **113**, 959–967

Blockade by dendrotoxin homologues of voltage-dependent K^+ currents in cultured sensory neurones from neonatal rats

Adam Hall, *John Stow, †Roger Sorensen, J. Oliver Dolly & [1]*David Owen

Department of Biochemistry, Imperial College of Science, Technology and Medicine, London, SW7 2AZ; *Wyeth Research (UK) Ltd., Taplow, Berkshire SL6 0PH and †Jefferson Medical College, Thomas Jefferson University, Philadelphia, PA 19107, U.S.A.

1 Homologues of dendrotoxin (Dtx) were isolated from the crude venom of Green and Black Mamba snakes and examined for K^+ channel blocking activity in neonatal rat dorsal root ganglion cells (DRGs) by whole-cell patch clamp recording.

2 Outward potassium current activated by depolarization was composed of two major components: a slowly inactivating current (SIC, $\tau_{decay} \approx 50$ ms, 200 ms and 2 s), and a non-inactivating current (NIC, $\tau_{decay} > 2$ min). Tail current analysis revealed two time constants of deactivation of total outward current, 3–12 ms and 50–150 ms (at −80 mV) which corresponded to SIC and NIC, respectively.

3 All the homologues (α-, β-, γ- and δ-Dtx and toxins I and K) blocked outward current activated by depolarization in a dose-dependent manner. The most potent in blocking *total* outward current was δ-Dtx (EC_{50} of 0.5 ± 0.2 nM), although there were no statistically significant differences in potency between any of the homologues.

4 Qualitative differences in the nature of the block were noted between homologues. In particular, the block by δ-Dtx was time-dependent, whereas that by α-Dtx was not.

5 α-Dtx was a much better blocker of SIC ($EC_{50} = 1.0 \pm 0.4$ nM) than was δ-Dtx ($EC_{50} = 17.6 \pm 5.8$ nM). Furthermore, δ-Dtx was selective for NIC ($EC_{50} \pm 0.24 \pm 0.03$ nM) over SIC and reduced the slow component of tail currents (NIC), preferentially. On the other hand, α-Dtx did not significantly distinguish between SIC and NIC although tail current analysis showed that α-Dtx preferentially reduced the fast component of tail currents (SIC).

6 The results confirm, using direct electrophysiological methods, that homologues of dendrotoxins from Mamba snake venom block K^+ channels in rat sensory neurones. Furthermore, α-Dtx and δ-Dtx distinguish between sub-types of K^+ channels in these cells and may thus be useful pharmacological tools in other neuronal K^+ channel studies.

Keywords: Dendrotoxins; potassium currents, dorsal root ganglion cells; neonatal rat

Introduction

The discovery of the naturally-occuring toxin, dendrotoxin (Harvey & Karlsson, 1980), in the venom of the Green Mamba snake (*Dendroaspis angusticeps*) provided a valuable tool for characterizing voltage-activated K^+ channels in neurones. Its usefulness arises from the fact that it is both highly potent and selective for a subset of voltage-activated K^+ channels. Since the initial separation of dendrotoxin (α-dendrotoxin or α-Dtx) from venom of the Green Mamba, a number of homologues, β_1-Dtx, β_2-Dtx, γ-Dtx and δ-Dtx, have also been isolated (Benishin *et al.*, 1988). In addition, closely-related peptides, Toxin I and K, have been purified from the Black Mamba (*Dendroaspis polylepis polylepis*) venom (Strydom, 1976). They are all basic polypeptides, containing ~60 amino acid residues that also show homology to Kunitz protease inhibitors (which are not themselves ion channel modulators) and to the smaller chain of β-bungarotoxin, a synaptically-active peptide from Krait venom (see Dolly, 1992). Most reports, to date, have indicated that α-Dtx is selective for delayed-rectifier-like K^+ currents, e.g. delayed rectifier K^+ currents in frog nerve fibres (Benoit & Dubois, 1986; Bräu *et al.*, 1990) and slowly- or non-inactivating outward K^+ conductances in sensory neurones of guinea-pigs and rats (Penner *et al.*, 1986; Stansfeld *et al.*, 1986; Stansfeld & Feltz, 1988). However, a Dtx-sensitive 'A-current' has been described in central CA1 neurones from rat and guinea-pig hippocampal slices (Halliwell *et al.*, 1986), although much higher concentrations and prolonged incubation times were required for an effect in this preparation.

Receptors for the dendrotoxins have been localized in the central nervous system (Pelchen-Matthews & Dolly, 1989) and purified from bovine brain (Parcej & Dolly, 1989). These are large sialoglyco-proteins containing α and β subunits of 65 kDa (after *N*-glycosylation) and 39 kDa, respectively. Microsequencing, by one group, of the N-terminus of the Dtx-purified α-subunit (Scott *et al.*, 1990), together with gene cloning (Reid *et al.*, 1992) has shown that this protein is homologous with a rat brain cloned K^+ channel, rKv1.2 (also known as RCK5), which is sensitive to α-Dtx when expressed in *Xenopus* oocytes (Stühmer *et al.*, 1989). Other microsequencing studies together with the use of specific antibodies suggest that Kv1.1 (also known as MK1, RCK1 and RBK1) channels also contribute to purified brain Dtx-binding protein (Rehm *et al.*, 1989). Kv1.1 cRNA + cDNA also gives rise to 'delayed-rectifier-like', Dtx-sensitive currents when expressed in *Xenopus* oocytes (Stühmer *et al.*, 1989) and mammalian cells (Owen *et al.*, 1992; Robertson & Owen, 1993; Bosma *et al.*, 1993).

It has been suggested that Dtx homologues can select for K^+ channel sub-types, although these conclusions were reached on the basis of indirect measurements (^{86}Rb efflux from synaptosomes) which lacked good temporal resolution (Benishin *et al.*, 1988). Other evidence in support of homologue-specific receptors has also been obtained from binding studies in synaptosomes (Muniz *et al.*, 1990) and autoradiographically in rat brain (Awan & Dolly, 1991). The present study is the first to examine directly, by electrophysiological methods, the actions of Dtx homologues on K^+ currents in mammalian neurones; namely rat dorsal root ganglion cells (DRGs). Two components of current were

[1] Author for correspondence.

characterized in these cells, a slowly-inactivating K^+ current (SIC) and a non-inactivating current (NIC). All the toxin homologues reduced the amplitude of the total outward K^+ current and evidence was found for selective block of the two components of K^+ current by α-Dtx and δ-Dtx, in particular. Some of the results of the present study have already been reported in preliminary form (Owen *et al.*, 1990; Hall *et al.*, 1991).

Methods

DRG cells were isolated from neonatal rats (1–3 days) and cultured for up to 5 days in accordance with previous methods (Wood *et al.*, 1988). In some cases, cells were replated in order to remove neurites thus facilitating whole-cell voltage-clamp. The bathing medium contained (mM): NaCl 124, KCl 2.5, $MgCl_2$ 4, HEPES 5, glucose 10, sucrose 20, pH 7.4; Tetrodotoxin (TTX) 1 μM was included to eliminate voltage-activated Na^+ currents and calcium omitted in order to minimize contaminating Ca^{2+} and Ca^{2+}-activated currents. Deactivation of outward K^+ currents was studied in a medium containing elevated K^+ (25 mM) in order to enhance the amplitude of tail currents recorded following repolarization.

Electrophysiological recordings were made by the whole-cell patch-clamp method with an Axoclamp 2A amplifier (Axon Instruments) in switch-clamp mode (5–7 kHz). Patch electrodes were prepared with a two-stage pull (Brown and Flaming), fire-polished and dipped in silane (Sigma) to reduce capacitance. Electrode resistance was typically 4–8 MΩ when filled with an intracellular medium consisting of (mM): Kgluconate 140, $MgCl_2$ 2, EGTA 1.1, HEPES 5, Glucose 16, pH 7.2. Individual cells were continually superperfused with bathing medium (30–40 μl min^{-1}) via a micro-perfusion system through which drugs were also applied. Raw data were acquired and analysed by M2-Lab (Instrutech Corp.) with an ITC-16 interface and Atari Mega ST4 computer. Currents were filtered at 1 kHz and sampled at between 0.1 ms and 0.5 ms per point. Data were subsequently analysed using REVIEW (Instrutech Corp.). Exponential analysis was carried out with REVIEW and other curve-fitting performed using IGOR (Wavemetrics) and NonLinII (Stephen Ikeda) on a Macintosh IIx. In some cases currents were digitally subtracted to isolate the inactivating components. Otherwise no leak subtraction of currents was carried out (leak $<5\%$ of non-inactivating outward current activated at +60 mV).

α-, β-, γ- and δ-Dtx were isolated from crude venom of *D. angusticeps* according to published methods (Benishin *et al.*, 1988; Dolly, 1992). The β-Dtx fraction was found to consist of a mixture of β_1- and β_2-Dtx by capillary electrophoresis. Toxins I and K were purified from the venom of *D. polylepis polylepis* by ultra-filtration, cation exchange chromatography, followed by reverse-phase high performance liquid chromatography (h.p.l.c.).

Results

Electrophysiological characterization of outward K^+ currents

Voltage-clamp experiments revealed that the total outward current was composed of at least two components. Depolarizing voltage steps from a holding potential of −40 mV elicited a non-inactivating current (NIC), whilst an additional slowly-inactivating current (SIC) was recruited with a hyperpolarizing pre-pulse to −100 mV (Figure 1a: inset). This was reflected in the current-voltage (*I-V*) relationships obtained under the two conditions (Figure 1a).

In some cells there was an initial inward current (within the first 50 ms) which was attributed to a TTX-resistant Na^+ current (Kostyuk *et al.*, 1981; Roy & Narahashi, 1992) since it was abolished by replacement of Na^+ by $Tris^+$ ions (not shown). The reversal potential (*ca.* −80 mV) of the outward current was consistent with that expected for a K^+ conductance. Typically a 1s test pulse yielded 5–10 nA of outward current (peak) which normally inactivated slowly (30–50%) over the time course of the step (Figure 1).

Activation and inactivation properties

The inactivating current (SIC) evoked by a depolarizing voltage step from −100 mV was isolated from the total outward current by subtracting NIC. Thereby, a series of such

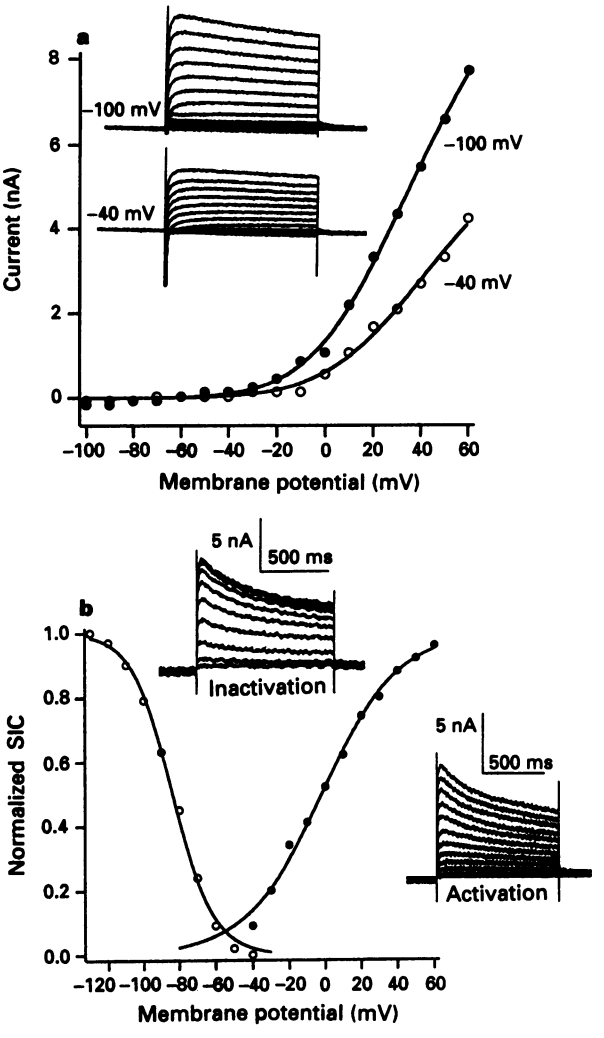

Figure 1 Inactivating and non-inactivating voltage-activated outward currents in dorsal root ganglia. (a) *Inset*: Raw current evoked with depolarizing voltage steps from holding potentiala of −100 mV (top panel) and −40 mV (lower panel). Tetrodotoxin (TTX)-resistant Na^+ currents are evident at the beginning of current records (truncated in upper traces). Current-voltage relationships constructed from the raw data: (○) −40 mV; (●) −100 mV. Additional current recruited by holding the cell at the more negative membrane potential. (b) activation and inactivation parameters of the slowly-inactivating current (SIC). The steady-state activation and inactivation curves were constructed from the peak values of difference currents (*insets*) which were obtained by subtracting the appropriate non-inactivating current (NIC) from the total outward currents measured at each voltage, as described in the Methods. The continuous lines drawn through the data points represent Boltzmann functions fitted to the raw data (inactivation: $V_h = -83.7$ mV, slope factor = 11.4 mV; activation: $V_h = -1.6$ mV, slope factor = 21.0 mV).

voltage steps were used to construct the steady-state activation- and inactivation-voltage relationships for SIC (Figure 1b). In the majority of cells, SIC was completely inactivated at between − 30 and − 40 mV. From the *I–V* curve for SIC, the threshold for activation of SIC was between − 50 mV and − 40 mV and a comparison of the *I-V* curves derived for SIC and total outward current suggested that NIC activated at more hyperpolarized potentials (− 70 mV to − 60 mV) (not shown).

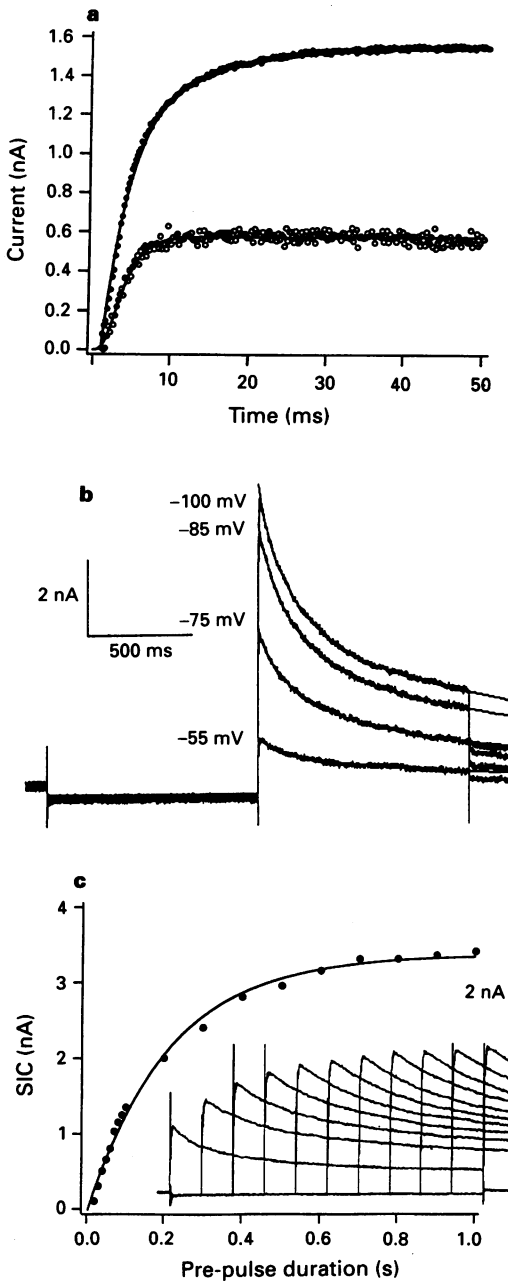

Figure 2 Kinetics of activation, inactivation and recovery from inactivation. (a) Currents were activated from a holding potential of − 30 mV or − 100 mV with a step to + 40 mV. Slowly inactivating current (SIC) was obtained by digital subtraction of current activated from − 30 mV (●). The non-inactivating current (NIC, ○), activated from − 30 mV, was leak subtracted (by scaling a − 10 mV hyperpolarizing pulse from − 60 mV). SIC (●) was fitted with a double exponential ($\tau_1 = 3.7$ ms, $\tau_2 = 14.6$ ms) with an offset of 2 ms. NIC (○) was fitted with a Hodgkin-Huxley function ($\tau = 0.5$ ms, $n = 4$). (b) SIC (obtained by subtraction) activated with a voltage step to + 60 mV following a pre-pulse (1 s) to membrane potentials indicated on the left. All the currents are fitted with a three component exponential function, the majority of the current in each case being described by the second and third components: − 55 mV (69 ms, 262 ms, 1.6 s); − 70 mV (47 ms, 239 ms, 1.8 s); − 85 mV (61 ms, 206 ms, 2.0 s); − 100 mV (53 ms, 203 ms, 2.1 s). (c) Recovery from inactivation at − 100 mV follows single exponential function ($\tau = 220$ ms). *Inset*: raw difference currents (*i.e.* difference between currents activated with and without prepulse to − 100 mV) vary with pre-pulse durations. Currents were activated at + 60 mV.

Activation kinetics

The time course of activation of SIC by a depolarizing step was best described by a double exponential function ($\tau_1 = 4$ ms, $\tau_2 = 15$ ms) following a brief delay (1.5 ms), whereas activation of NIC followed a sigmoidal time course which was well fitted by the Hodgkin-Huxley equation ($n = 4$ and $\tau = 0.5$ ms) (Figure 2a).

Inactivation

Inactivation of SIC was in most cases adequately described by the sum of three exponential components ($\tau_1 = 20$–80 ms,

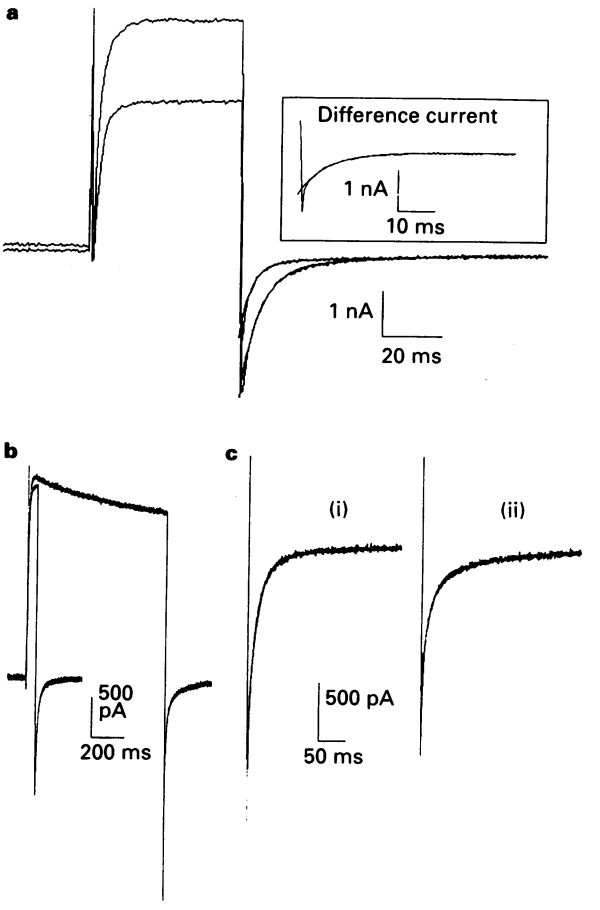

Figure 3 Inactivating current deactivates according to a single exponential. (a) Currents activated at + 40 mV either from − 80 mV (upper trace) or − 30 mV (lower trace). Tail currents measured following repolarization to − 80 mV decay according to a double or single exponential process, respectively. The tail currents have been fitted (fitted curve superimposed upon raw data) and parameters of 3.5 ms, 1.9 nA and 49 ms, 0.3 nA obtained for current activated from − 30 mV, whereas tail currents following current activated from − 80 mV gave parameters of: 6 ms, 3.2 nA and 99 ms, 0.3 nA. Tail current of the difference current (corresponding to the inactivating component of outward current) was fitted with a single exponential function ($\tau = 6.8$ ms). (b) Tail currents measured at 50 ms or 750 ms after activation of outward current at + 40 mV. (c) Tail currents as in (b) but shown on a faster sweep, (i) t = 50 ms, (ii) t = 750 ms. Double exponential fits are superimposed on the raw data. Parameters: 11.0 ms, 1.40 nA and 130 ms, 0.11 nA (t = 50 ms); 10.5 ms, 0.88 nA and 135 ms, 0.26 nA (t = 750 ms).

τ_2 = 200–300 ms and τ_3 = 1–3 s). The time-course of inactivation was not influenced by pre-pulse potential, between − 50 and − 100 mV, indicating that no additional currents were recruited over this range of membrane potentials (Figure 2b).

Recovery from inactivation of SIC followed a single exponential function (τ = 220 ms at − 100 mV, Figure 2c, the rate of which was voltage-sensitive (*eg.* at − 20 mV recovery was complete only after *ca.* 10 s; not shown). An anomalous decrease in amplitude of the activated current following

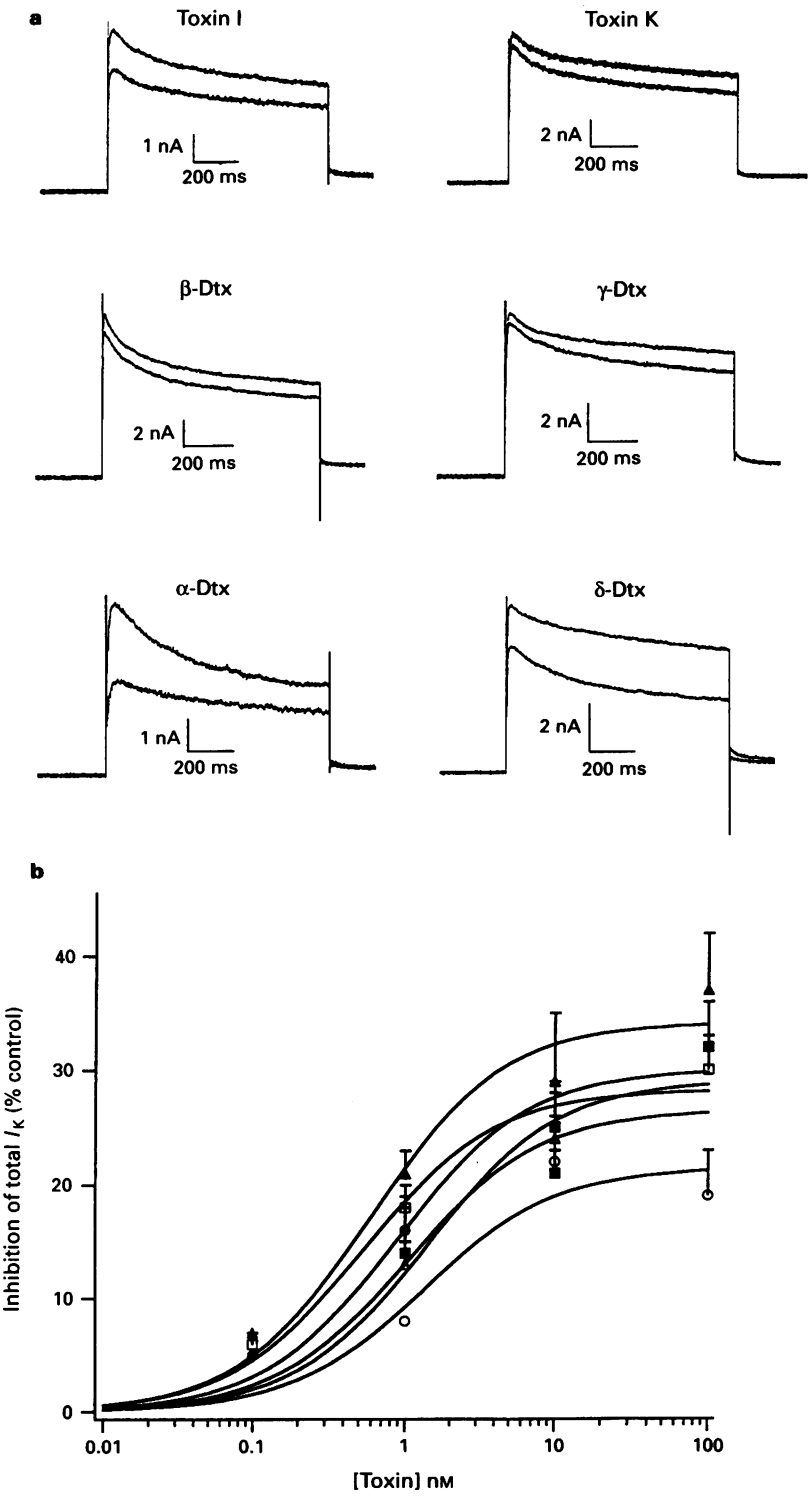

Figure 4 Block of voltage-activated currents in dorsal root ganglia cells by dendrotoxin homologues. (a) Dendrotoxin homologues from Black and Green Mamba venom applied by local perfusion at a concentration of 10 nM in each case. All homologues blocked voltage-activated K^+ current to some degree with variation in the extent of inhibition. In each panel two current records are shown overlaid, a control and one taken in the presence of a dendrotoxin homologue. All currents were activated with a voltage step to + 60 mV from a conditioning potential of − 100 mV. (b) Dose-response relationships constructed using the amount of inhibition of current at the end of voltage-steps by toxin. Data have been fitted with the logistic function and EC_{50}s derived from the equation: $y = y_{max}/1 + (EC_{50}/[toxin])^n$. EC_{50}s were: α-Dtx (●), 0.87 ± 0.35 nM; β-Dtx (○), 1.33 ± 1.11 nM; γ-Dtx (■), 1.39 ± 1.29 nM; δ-Dtx (□), 0.52 ± 0.18 nM; Toxin I (▲), 0.59 ± 0.27 nM; Toxin K (△), 1.04 ± 0.60 nM. S.e.means shown for n = 4–6. Bars represent s.e.mean, n = 4–6.

hyperpolarizations of up to 30 ms in duration occurred before subsequently increasing with more prolonged conditioning steps (not shown). In subsequent experiments, in order that inactivation be removed fully, a 1 s hyperpolarizing pre-pulse was employed.

Deactivation

The tail currents recorded at − 80 mV, following activation of outward currents at + 40 mV, decayed according to the sum of two exponential functions ($\tau_1 = 3-12$ ms and ($\tau_2 = 50-150$ ms: Figure 3a). The fast component was preferentially reduced when the holding potential was depolarized (*e.g.* − 30 mV) and indeed difference currents obtained under these circumstances could be fitted quite well by a single exponential function with time constant of 6.8 ms (Figure 3a: inset). Similarly, the fast component of the tail current was preferentially reduced following longer steps (Figure 3b and c). Thus tail current analyses indicated that SIC and NIC deactivate according to the fast and slow time constants, respectively.

Inhibition of voltage-activated K^+ currents by Dtx homologues

α-, β-, γ- and δ-Dtx homologues from *D. angusticeps* venom, and Toxins I and K from *D. polylepis polylepis* venom, exhibited a spectrum of activities on the outward K^+ current activated from − 100 mV (Figure 4). All the homologues were found to block outward current in a dose-dependent fashion and to varying degrees. The onset of inhibition by toxins was relatively quick, taking 1–2 min to reach steady-state. However, recovery from block by toxins was rarely complete. Typically 80–90% of the total outward current remained although the actual extent of washout and time taken to recover was dependent upon length of exposure and

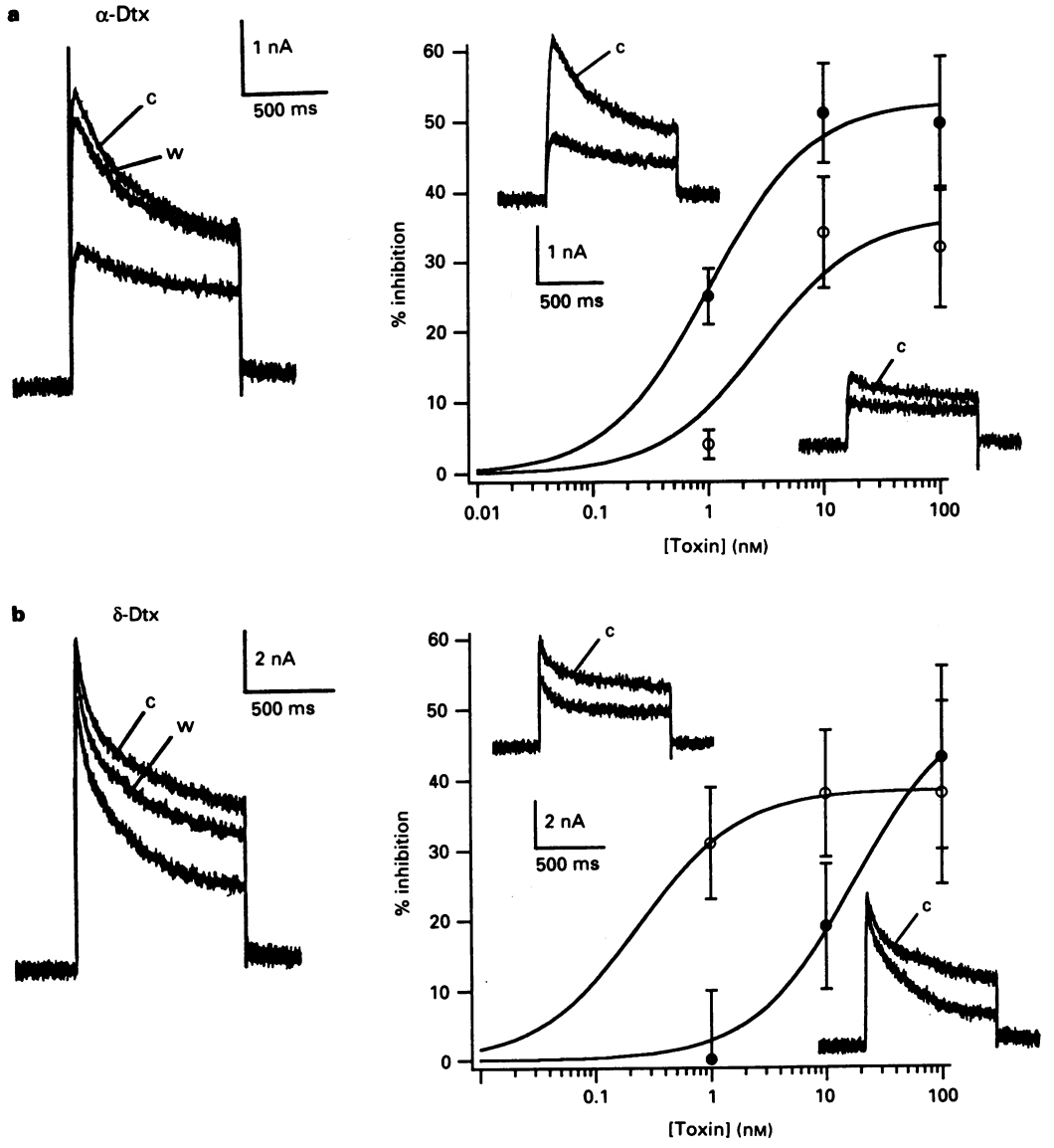

Figure 5 Differential block of slowly inactivating currents (SIC) and non-inactivating currents (NIC) by α-Dtx and δ-Dtx. Dose-response relationships for block of NIC and SIC by α-Dtx (a) and δ-Dtx (b). *Left*: whereas α-Dtx (10 nM) blocks a similar proportion of current at the beginning and end of the step, δ-Dtx (10 nM) shows time-dependent block. *Right*: Dose-response relationships for block of NIC (○) and SIC (●) components of current determined from difference currents (Methods). In each panel, insets are juxtaposed with the relevant dose-response curve *e.g.* top panel: top left insets are SIC currents (● in graph) and bottom right insets are NIC currents (○ in graph). In each case 'c' indicates the control current and 'w' the current after washout. Current amplitudes were measured at the end of voltage-steps and curves drawn according to the logistic function, from which EC_{50}s were derived: α-Dtx, 1.0 ± 0.4 nM and 2.9 ± 3.5 nM for SIC and NIC respectively; δ-Dtx, 17.6 ± 5.8 nM and 0.24 ± 0.03 nM for SIC and NIC, respectively. Bars represent s.e.mean, $n = 3-4$.

degree of block. For example, for a 1–3 min application of 10 nM α-Dtx, washout took *ca.* 5 min, whereas further irreversible inhibition was obtained by continued application of toxin for up to 10 min. Interestingly, the maximum amount of block achievable was *ca.* 30–40% of the control peak current (see graph, Figure 4b), although in some cells subjected to a more prolonged exposure (up to 10 min), the steady-state block by 10 nM α-Dtx reached *ca.* 50–70% of total current. In these cases only partial recovery was observed and an underlying rundown of the K^+ current, seen in other cells (10–20% over *ca.* 30 min), may have contributed to the observation.

Dose-reponse curves to each of the toxin homologues were fitted with the logistic function and EC_{50}s were thus derived (Figure 4b). δ-Dtx had the lowest EC_{50} (0.52 ± 0.18 nM), however although a factor of about 2.7 separated the EC_{50}s of the most and least active homologues, there were in fact no statistically-significant differences in the apparent potency in blocking the total outward currents.

Qualitative differences in the nature of block were observed in some cases. For example, the proportion of current blocked by 10 nM α-Dtx and Toxin I was constant throughout the duration of the step, whereas the effect of δ-Dtx was time-dependent, resulting in more inhibition at the end of the step than immediately after the depolarizing voltage jump (Figure 4a). A tendency for Toxin K and β- and γ-Dtx to behave in this way was also seen, although in these cases the response was much less clear-cut and was not studied further. The qualitative difference in the mode of block seen with α-Dtx and δ-Dtx, prompted an examination of whether it could be ascribed to a selective action on different components of K^+ current or, alternatively, differences in the mechanism of block.

Selective blockade of K^+ currents by dendrotoxin homologues

Difference currents In order to isolate the inactivating (SIC) and non-inactivating (NIC) currents, cells were held at − 30 mV or − 40 mV and currents activated with depolarizations to + 60 mV with or without a one second hyperpolarizing pre-pulse to − 100 mV (*e.g.* Figure 3a).

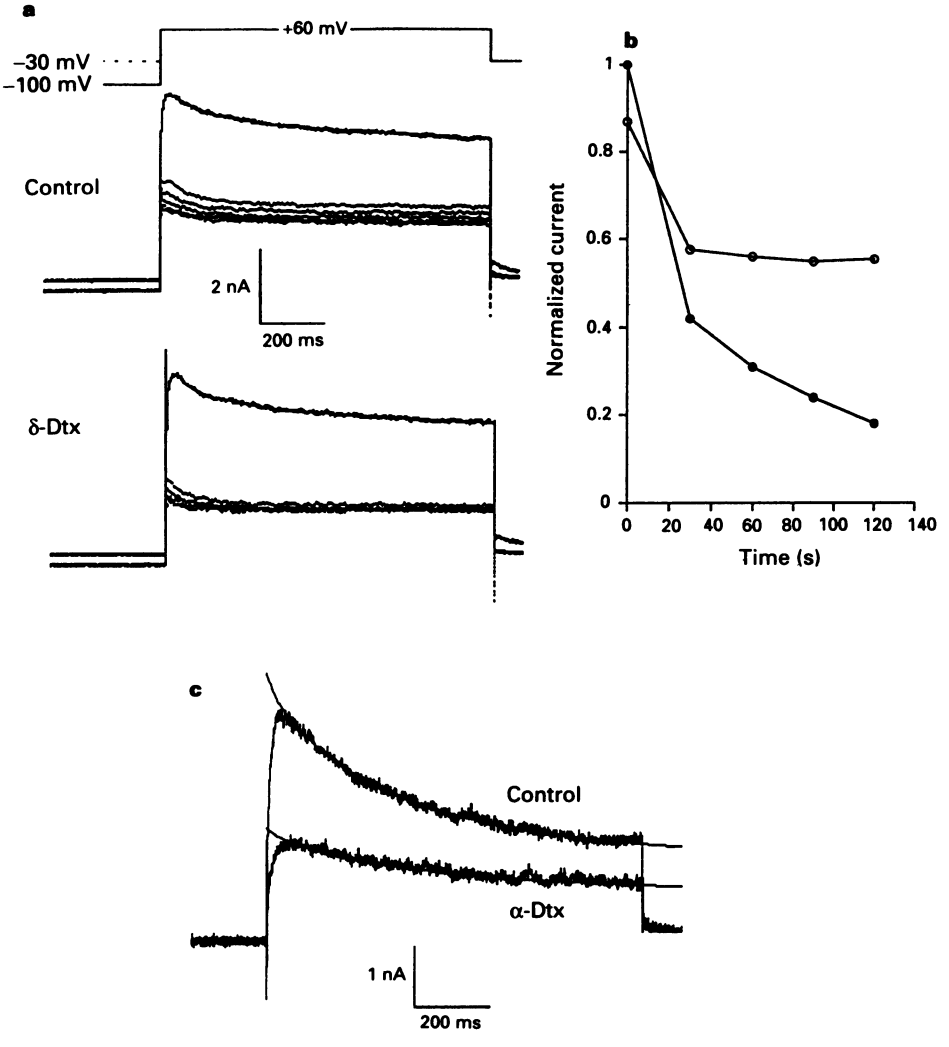

Figure 6 Effects of δ-Dtx and α-Dtx on inactivation of slowly inactivating current (SIC). (a) Series of currents evoked with a voltage step to + 60 mV before and during application of 3 nM δ-Dtx. First current in each series (largest) evoked following a condition step to − 100 mV. Current then declined with successive test depolarizations, the residual current representing non-inactivating current (NIC). (b) SIC (●) (normalized with respect to maximum amplitude) *vs* time to illustrate slow inactivation; (○) ratio of currents obtained *following* the conditioning pulse (to − 100 mV), in the presence and absence of δ-Dtx. The ratio decreases during the first 30 s but remains constant thereafter even though slow inactivation of SIC is not complete. (c) Two difference currents (SIC), superimposed, in the presence and absence of 10 nM α-Dtx. Although αDtx blocks *ca.* 50% of the current, there is no effect on the rate of decay. The two currents have been fitted with a three component exponential in each case having the parameters: control, 0.27 nA, $\tau_1 = 22.5$ ms; 1.97 nA, $\tau_2 = 238.0$ ms; 1.95 nA, $\tau_3 = 4.15$s; α-Dtx, 0.08 nA, $\tau_1 = 24.1$ ms; 0.69 nA, $\tau_2 = 269.0$ ms; 1.14 nA, $\tau_3 = 4.01$ s.

At low concentrations (*e.g.* 1 nM), α-Dtx was virtually selective for SIC and even at higher concentrations blocked SIC in preference to NIC. For example, in Figure 5a, 10 nM α-Dtx reduced SIC by *ca.* 60% compared with *ca.* 30% inhibition of NIC (leak current *ca.* 2% of control). Toxin I (1 nM) showed a similar selectivity of action (not shown). In contrast to α-Dtx, the overall effect of δ-Dtx on total outward current was very time-dependent (Figure 5b). Low concentrations of δ-Dtx (*e.g.* 1 nM) selectively blocked NIC although higher concentrations also blocked SIC to a variable degree (Figure 5b: inset). The voltage-dependence that gave rise to the observed time-dependent block, on occasion gave rise to an apparent *increase* in the amount of SIC, although evidently there was an *overall decrease* in total outward current (not shown). This selectivity for SIC and NIC by α-Dtx and δ-Dtx respectively, was reflected in the *I-V* relationships for α-Dtx and δ-Dtx-sensitive currents, which revealed δ-Dtx-sensitive current at more negative potentials (not shown).

These relationships indicate an equipotent molar ratio (e.p.m.r.) for α-Dtx over δ-Dtx of *ca.* 0.06, with respect to SIC, and 12.25 with respect to NIC. Although α-Dtx was apparently selective for SIC over NIC e.p.m.r. = 0.35), this was not statistically significant. On the other hand, δ-Dtx was selective for NIC over SIC (e.p.m.r. *ca.* 0.01). The maximum amount of block of SIC and NIC was similar for α-Dtx (53% and 36%, respectively) and δ-Dtx (51% and 38%, respectively).

Block by α-Dtx was not voltage-dependent having a negligible effect on the conductance-voltage relationship ($V_{1/2}$ shifted from + 5 mV to + 1 mV) (not shown). Furthermore, there was no effect of α-Dtx on the rate of inactivation of SIC (Figure 6c).. δ-Dtx (3 nM), on the other hand, clearly accelerated the decay of the total outward current (Figure 5b). This did not result from an acceleration of slow inactivation as indicated by the fact that the ratio of currents in the absence and presence of δ-Dtx reached a minimum within 30 s and was constant thereafter. In contrast slow inactivation was not complete until 2–3 min had elapsed (Figure 6b). Rather, it is likely that the time-dependent action of δ-Dtx reflects an open-channel type of block which is relieved at negative potentials.

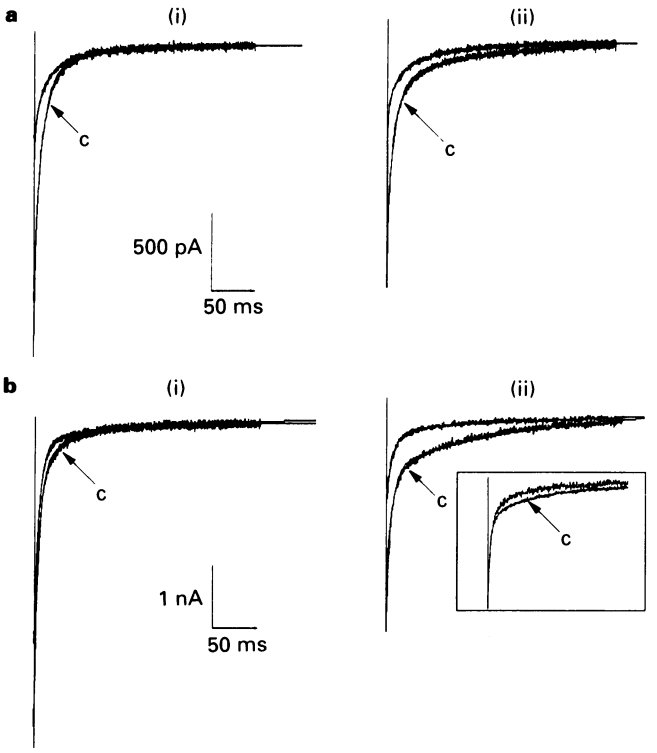

Figure 7 α-Dtx and δ-Dtx block different components of tail currents. Tail currents recorded in presence and absence of 3 nM α-Dtx (a) and 3 nM δ-Dtx (b). Tail currents were measured 50 ms (*i*) or 750 ms (*ii*) after activation (at + 40 mV) of outward current at a reference potential of − 80 mV. In each case (*c*) indicates the control current. Tail currents are fitted with double exponential functions: (a) (i) control: 0.18 nA, $\tau_1 = 63$ ms, 1.44 nA, $\tau_2 = 8.9$ ms; α-Dtx: 0.2 nA, $\tau_1 = 46.8$ ms, 0.38 nA, $\tau_2 = 9.8$ ms; (a) (ii) control: 0.28 nA, $\tau_1 = 128$ ms, 1.04 nA, $\tau_2 = 8.3$ ms; α-Dtx: 0.18 nA, $\tau_1 = 161$ ms, 0.33 nA, $\tau_2 = 11.1$ ms; (b) (i) control: 0.66 nA, $\tau_1 = 59.2$ ms, 4.2 nA, $\tau_2 = 5.1$ ms; δ-Dtx; 0.3 nA, $\tau_1 = 115$ ms, 3.2 nA, $\tau_2 = 5.6$ ms; (b) (ii) control: 0.91 nA, $\tau_1 = 141$ ms, 1.8 nA, $\tau_2 = 5.9$ ms; δ-Dtx: 0.31 nA, $\tau_1 = 234$ ms, 1.1 nA, $\tau_2 = 7.7$ ms. *Insert*: tail current in δ-Dtx scaled (× 2.4) to match peak of control tail current.

Tail currents

As shown by difference current analysis, α-Dtx and δ-Dtx were apparently selective for SIC and NIC, respectively. This conclusion was supported by the observation that the fast component of the tail current, which was associated with SIC (see above), was more sensitive to inhibition by α-Dtx than the slow component (Figure 7a). In contrast, the slow component of the tail current, which was attributed to deactivation of NIC, was preferentially reduced by δ-Dtx (Figure 7b).

For example, following activation to + 40 mV for 50 ms, α-Dtx (3 nM) reduced the fast component of deactivation ($\tau = 8.9–9.8$ ms) by 74%, whereas the amplitude of the slow component ($\tau = 47–62$ ms) remained relatively unaffected. Curiously, α-Dtx decreased the amplitude of the slow tail current, measured at $t = 750$ ms, although this was not as substantial an effect as the block of the fast component. In contrast, the principle effect of δ-Dtx (3 nM) was to decrease the amplitude of the slow component (55%, compared with a 24% reduction in the fast component). This effect was time-dependent, being more evident after longer voltage steps (Figure 7b). Interestingly, both α-Dtx and δ-Dtx appeared to slow the decay of the slow component of tail currents.

Discussion

Receptors for the K^+ channel toxins, α-Dtx, δ-Dtx and Toxin I, have been extensively characterized in neuronal tissue (Black *et al.*, 1988; Rehm & Lazdunski, 1988; Muniz *et al.*, 1990). With the exception of α-Dtx and Toxin I, functional activity of other Dtx homologues has so far only been studied against cloned K^+ channels (Kavanaugh *et al.*, 1990; Owen *et al.*, 1992) or indirectly, by monitoring ^{86}Rb efflux from rat brain synaptosomes (Benishin *et al.*, 1988; Sorensen *et al.*, 1990). The results of the latter experiments were interpreted as evidence of homologue selectivity for subtypes of voltage-activated K^+ channel (Benishin *et al.*, 1988). The results of the present study also suggest specificity of various homologues for sub-types of K^+ channel, although the details differ markedly from those of the above study.

We have identified two distinct components of voltage-activated K^+ current, a slowly-inactivating current (SIC) and a non-activating current (NIC). This was deduced from the following observations: (1) depolarized holding potentials inactivated a proportion of the total outward current activated by depolarizing voltage steps; (2) kinetic analysis showed that the activation of SIC and NIC were different; (3) tail current analysis revealed two exponential processes, consistent with the deactivation of two types of K^+ channel.

All the homologues blocked a fraction of the total voltage-activated K^+ current in these cells at concentrations in the range 1 nM–1 μM. The most potent of the homologues was δ-Dtx (EC_{50} *ca.* 0.5 nM) although the apparent differences between homologues in their ability to block *total* outward currents were not statistically significant. In all cases the toxin homologues blocked at most only *ca.* 35% of the total K^+ current, even at concentrations up to 1 μM (not shown). Furthermore, even with subtracted currents the maximum

amount of block was only *ca.* 50% (*e.g.* α-Dtx *vs.* SIC). This inability of dendrotoxins to block all of SIC or NIC might reflect an inherent property of the toxin-channel interaction. This seems unlikely since Dtx homologues cause almost complete block (up to 90%) of heterologously- (and singly-) expressed cloned K^+ α-subunits, such as mKv1.1 (Owen *et al.*, 1992). However, combinations of K^+ channel α-subunit sub-types into hetero-oligomeric structures may occur in the DRG, as has been found in various other neuronal preparations (Sheng *et al.*, 1993; Wang *et al.*, 1993; Scott *et al.*, 1994). Indeed at least four members of the Kv1 class K^+ channels are expressed in rat DRGs, including the Dtx-sensitive α-subunits: rKv1.1 (RCK1) and rKv1.2 (RCK5) and the Dtx-insensitive channels: rKv1.3 (RCK3) and rKv1.4 (RCK4) (Beckh & Pongs, 1990). *In vitro*, mixing and matching of subunits results in mixed properties although not in a predictable manner (Po *et al.*, 1993) and it is conceivable that the ceiling on block results from such a combination. An alternative explanation for this observation is that at a molecular level, SIC (*e.g.*) may comprise more than one species of inactivating channel which have varying sensitivity to dendrotoxins but are nevertheless isolated together on the basis of similar electrophysiological characteristics. Note, however that the association of single tail currents with SIC does not support this idea.

α- and δ-Dtx had qualitatively distinct blocking characteristics which implied different mechanisms of action. In particular, the block by δ-Dtx was voltage- and time-dependent, whereas the block by α-Dtx was neither. Furthermore as shown by both difference current and tail current analyses, α-Dtx and δ-Dtx selectively blocked SIC and NIC, respectively. The time-dependence of the block by δ-Dtx is consistent with an open-channel blocking mechanism and relief at hyperpolarized potentials in the continued presence of the toxin. The 'slow inactivation' of SIC (time course *ca.* 2.5 to 3 min) was unaffected by δ-Dtx since normalized (ratioed) currents remained constant after the initial 30 s. No growth phase was seen in the tail currents which could be ascribed to unblocking of channels, although there *was* an increase in the amplitude and time constant of decay of the slow component of the tail current in the presence of 3 nM δ-Dtx which could reflect such a phenomenon. The lack of time-dependence to the block by δ-Dtx of currents activated from −30 mV may reflect the fact that NIC is already at least partially activated at this potential.

These electrophysiological results suggest that α-Dtx and δ-Dtx have specificity for distinct subtypes of K^+ currents, although single channel recording is required to confirm such an interpretation. Support for this notion does come, however, from biochemical studies on toxin binding sites (Dolly, 1992) which suggest that δ-Dtx can distinguish between two α-Dtx receptors from bovine brain. At low concentrations (*e.g.* 1 nM, as used in this study), only one of these sites was labelled by δ-Dtx. Co-distribution of α-Dtx and δ-Dtx sites and mutual antagonism of their binding has been described in rat brain sections (Awan & Dolly, 1991) and it is tempting to speculate that this common acceptor might correspond to NIC. The weak affinity of δ-Dtx for the second population of α-Dtx acceptor, suggests that this site may reside on SIC channels, in view of the relatively weak block of this current by δ-Dtx. Additional support for the existence of distinct sites of action of α-Dtx and δ-Dtx is lent by the observation that α-Dtx, but not δ-Dtx, enhances electrically evoked noradrenaline release in rat hippocampus (Hu *et al.*, 1991). Furthermore, cloned rat brain K^+ channels from the *Shaker* sub-family (rKv1.1, rKv1.2 & rKv1.6), exhibit differential sensitivity to dendrotoxin homologues, when expressed in *Xenopus* oocytes: specifically, δ-Dtx is the more potent blocker of rKv1.1 (Kavanaugh *et al.*, 1990; Wittka & Pongs, personal communication) whereas against rKv1.2, the rank order is reversed and α-Dtx is more potent (Wittka & Pongs, personal communication). We therefore, tentatively suggest that NIC and SIC may represent rKv1.1 and rKv1.2, respectively.

The dendrotoxins share considerable sequence homology (Dufton, 1985; Harvey & Karlsson, 1982). Whereas the C-terminus is highly conserved (including the electrophysiologically-inactive protease-inhibitors). (Joubert & Taljaard, 1980; Dufton, 1985), the N-terminus of α-Dtx, Toxin I, δ-Dtx, Toxin K, β-Dtx and γ-Dtx varies significantly (Benishin *et al.*, 1988) and thus may be important in determining channel specificity. Several clusters of positively-charged residues are represented in all the homologues but with subtle variations. For example, δ-Dtx has three consecutive lysines at positions 17, 18 and 19, whereas Toxin K has two ($Lys^{17\ \&\ 19}$) and α-Dtx and Toxin I have only a one (Lys^{19}) in this region. Other regions of possible significance include a triplet of lysines in α-Dtx and Toxin I ($Lys^{28,\ 29\ \&\ 30}$) which lie on a protruding loop connecting two β-sheets in the tertiary structure (Skarzynski, 1992) and which is represented by only Lys^{28} & Lys^{30} in δ-Dtx and Toxin K. In addition, α-Dtx has three positively-charged residues (Arg^3, Arg^4 and Lys^5) at the N-terminus, whereas δ-Dtx has only one, Lys^5. Chemical modification of dendrotoxin also indicates that a positively charged residue at position 3 and residues around position 17 are important for biological activity (Hollecker *et al.*, 1993). The results obtained in the present study suggest that dendrotoxin homologues, in particular α-Dtx and δ-Dtx, may be useful pharmacological tools in the study of neuronal subtypes of voltage-activated K^+ channels. Further studies of the interactions of Dtx homologues with cloned K^+ channels, together with single channel recording in neurones, will be needed to determine the precise mechanisms underlying the different properties of α-Dtx and δ-Dtx observed here.

This study was funded in part by the Medical Research Council. A.H. was in receipt of an SERC-Wyeth Research (UK), CASE-studentship. We wish to thank David Parcej (Imperial College) and Zilda Muniz (Imperial College) for providing us with purified α-Dtx and purified δ-Dtx, respectively and Nadine Bissue (Wyeth Research) and Janette Scott (Wyeth Research) for the isolation and maintenance of DRGs in tissue culture.

References

AWAN, K.A. & DOLLY, J.O. (1991). K^+ channel sub-types in rat brain: characteristic locations revealed using β-bungarotoxin, α- and δ-dendrotoxins. *Neurosci.*, **40**, 29–39.

BECKH, S. & PONGS, O. (1990). Members of the RCK potassium channel family are differentially expressed in the rat nervous system. *EMBO. J.*, **9**, 777–782.

BENISHIN, C.G., SORENSEN, R.G., BROWN, W.E., KRUEGER, B.K. & BLAUSTEIN, M.P. (1988). Four polypeptide components of green mamba venom selectively block certain potassium channels in rat brain synaptosomes. *Mol. Pharmacol.*, **34**, 152–159.

BENOIT, E. & DUBOIS, J.-M. (1986). Toxin I from the snake *Dendroaspis polylepis polylepis*: a highly specific blocker of one type of potassium channel in myelinated nerve fiber. *Brain Res.*, **377**, 374–377.

BLACK, A.R., DONEGAN, C.M., DENNY, B.J. & DOLLY, J.O. (1988). Solubilization and physical characterisation of acceptors for dendrotoxin and β-bungarotoxin from synaptic membranes of rat brain. *Biochem.*, **27**, 6814–6820.

BOSMA, M.M., ALLEN, M.L., MARTIN, T.M. & TEMPEL, B.L. (1993). PKA-dependent regulation of mKv1.1, a mouse *Shaker*-like potassium channel gene, when stably expressed in CHO cells. *J. Neurosci.*, **13**, 5242–5250.

BRÄU, M.E., DREYER, F., JONAS, P., REPP, H. & VOGEL, W. (1990). A K^+ channel in *Xenopus* nerve fibres selectively blocked by bee and snake toxins: binding and voltage-clamp experiments. *J. Physiol.*, **420**, 365–385.

DOLLY, J.O., PARCEJ, D.N., SCOTT, V.E., MUNIZ, Z.M., SEWING, S. & PONGS, O. (1992). Molecular architecture of K^+ channels. *Neurochem. Int.*, (in press).

DUFTON, M.J. (1985). Proteinase inhibitors and dendrotoxins. *Eur. J. Biochem.*, **153**, 647–654.

HALL, A., STOW, J., DOLLY, O. & OWEN, D.G. (1991). Dendrotoxin homologues block voltage-dependent potassium currents in cultured rat dorsal root ganglion cells by different mechanisms. *10th World Congress on Animal, Plant & Microbial Toxins*, Abstr. 371.

HALLIWELL, J.V., OTHMAN, I.B., PELCHEN-MATTHEWS, A. & DOLLY, J.O. (1986). Central action of dendrotoxin: selective reduction of a transient K^+ conductance in hippocampus and binding to localised acceptors. *Proc. Natl. Acad. Sci. U.S.A.*, **83**, 493–497.

HARVEY, A.L. & KARLSSON, E. (1980). Dendrotoxin from the venom of the green mamba, *Dendroaspis angusticeps*. A neurotoxin that enhances the acetylcholine release at neuromuscular junctions. *Naunyn-Schmied. Arch. Pharmacol.*, **312**, 1–6.

HARVEY, A.L. & KARLSSON, E. (1982). Protease inhibitor homologues from mamba venoms: facilitation of acetylcholine release and interactions with prejunctional blocking toxins. *Br. J. Pharmacol.*, **77**, 153–161.

HOLLECKER, M., MARSHALL, D.L. & HARVEY, A.L. (1993). Structural features important for the biological activity of the potassium channel blocking dendrotoxins. *Br. J. Pharmacol.*, **110**, 790–794.

HU, P.S., BENISHIN, C. & FREDHOLM, B.B. (1991). Comparison of the effects of four dendrotoxin peptides, 4-aminopyridine and tetraethylammonium on the electrically-evoked [^{3}H]noradrenaline release from rat hippocampus. *Eur. J. Pharmacol.*, **209**, 87–93.

JOUBERT, F.J. & TALJAARD, N. (1980). The amino acid sequence of two proteinase inhibitor homologues from *Dendroaspis angusticeps* venom. *Hoppe-Seyler's Z. Physiol. Chem.*, **361**, 661–674.

KAVANAUGH, M.P., OSBORNE, P.B., CHRISTIE, M.J., BUSCH, A.E., HARTSHORNE, R.P., NORTH, R.A. & ADELMAN, J.P. (1990). Sensitivity to blocking agents of cloned potassium channels expressed in *Xenopus* oocytes. *Soc. Neurosci. Abstr.*, **16**, Abstr. 281.14.

KOSTYUK, P.G., VESELOVSKY, N.S. & TSYNDRENKO, A.Y. (1981). Ionic currents in the somatic membrane of rat dorsal root ganglion neurons-I. Sodium currents. *Neurosci.*, **6**, 2423–2430.

MUNIZ, Z.M., DINIZ, C.R. & DOLLY, J.O. (1990). Characterization of binding sites for δ-dendrotoxin in guinea-pig synaptosomes: relationship to acceptors for the K^+-channel probe α-dendrotoxin. *J. Neurochem.*, **54**, 343–346.

OWEN, D.G., HALL, A., SORENSEN, R.G. & STOW, J. (1990). Inhibition of outward currents in dorsal root ganglion cells by dendrotoxin homologues. *Soc. Neurosci. Abstr.*, **16**, Abstr. 156.8.

OWEN, D.G., ROBERTSON, B., HALL, A. & SCOTT, J.A. (1992). Blockade by peptidic toxins of MK1 potassium currents in CHO cells. *Soc. Neurosci. Abstr.*, **18**, Abstr. 335.1.

PARCEJ, D.N. & DOLLY, J.O. (1989). Dendrotoxin acceptor from bovine synaptic plasma membranes: binding properties, purification and subunit composition of a putative constituent of certain voltage-activated K^+ channels. *Biochem. J.*, **257**, 899–903.

PELCHEN-MATTHEWS, A. & DOLLY, J.O. (1989). Distribution in the rat central nervous system of acceptor sub-types for dendrotoxin, a K^+ channel probe. *Neuroscience*, **29**, 347–361.

PENNER, R., PETERSEN, M., PIERAU, F.-K. & DREYER, F. (1986). Dendrotoxin: a selective blocker of a non-inactivating potassium current in guinea-pig doral root ganglion neurones. *Pflüger's Arch.*, **407**, 365–369.

PO, S., ROBERDS, S., SYNDERS, D.J., TAMKUN, M.M. & BENNETT, P.B. (1993). Heteromultimeric assembly of human potassium channels. Molecular basis of a transient outward current? *Circ. Res.*, **72**, 1326–1336.

REHM, H. & LAZDUNSKI, M. (1988). Purification and subunit structure of a putative K^+ channel protein identified by its binding properties for dendrotoxin I. *Proc. Natl. Acad. Sci. USA*, **85**, 4919–4923.

REHM, H., NEWITT, R.A. & TEMPEL, B.L. (1989). Immunological evidence for a relationship between the dendrotoxin-binding protein and the mammalian homologue of the *Drosophila Shaker* K^+ channel. *FEBS Lett.*, **249**, 224–228.

REID, P.F., PONGS, O. & DOLLY, J.O. (1992). Cloning of a bovine voltage-gated K^+ channel gene utilising partial amino acid sequence of a dendrotoxin-binding protein from brain cortex. *FEBS Lett.*, **302**, 31–34.

ROBERTSON, B. & OWEN, D.G. (1993). Pharmacology of a cloned potassium channel from mouse brain (MK-1) expressed in CHO cells: effects of blockers and an inactivation peptide. *Br. J. Pharmacol.*, **109**, 725–735.

ROY, M.L. & NARAHASHI, T. (1992). Differential properties of tetrodotoxin-sensitive and tetrodotoxin-resistant sodium channels in rat dorsal root ganglion neurons. *J. Neurosci.*, **12**, 2104–2111.

SCOTT, V.E.S., PARCEJ, D.N., KEEN, J.N., FINDLAY, J.B.C. & DOLLY, J.O. (1990). α-dendrotoxin acceptor from bovine brain is a K^+ channel protein: evidence from the N-terminal sequence of its larger subunit. *J. Biol. Chem.*, **265**, 20094–20097.

SCOTT, V.E.S., MUNIZ, Z.M., SEWING, S., LICHTINGHAGEN, R., PARCEJ, D.N., PONGS, O. & DOLLY, J.O. (1994). Antibodies specific for distinct K_v subunits unveil a heterooligomeric basis for subtypes of α-dendrotoxin-sensitive K^+ channels in bovine brain. *Biochemistry*, **33**, 1617–1623.

SHENG, M., LIAO, Y.J., JAN, Y.N. & JAN, L.Y. (1993). Presynaptic A-current based on heteromultimeric K^+ channels detected *in vivo*. *Nature*, **365**, 72–75.

SKARZYNSKI, T. (1992). Crystal structure of α-dendrotoxin from the green mamba venom and its comparison with the structure of bovine pancreatic trypsin inhibitor. *J. Mol. Biol.*, **224**, 671–683.

SORENSEN, R.G., SCHNEIDER, M.J., ROGOWSKI, R.S. & BLAUSTEIN, M.P. (1990). Snake and scorpion neurotoxins as probes of rat brain synaptosomal potassium channels. *Prog. Clin. Biol. Res.*, **334**, 279–301.

STANSFELD, C.E., MARSH, S.J., HALLIWELL, J.V. & BROWN, D.A. (1986). 4-aminopyridine and dendrotoxin induce repetitive firing in rat visceral sensory neurones by blocking a slowly inactivating outward current. *Neurosci. Lett.*, **64**, 299–304.

STANSFELD, C. & FELTZ, A. (1988). Dendrotoxin-sensitive K^+ channels in dorsal root ganglion cells. *Neurosci. Lett.*, **93**, 49–55.

STRYDOM, D.J. (1976). Snake venom toxins. Purification and properties of low-molecular weight polypeptides of *Dendroaspis polylepis* (Black Mamba) venom. *Eur. J. Biochem.*, **69**, 169–176.

STÜHMER, W., RUPPERSBERG, J.P., SCHRÖTER, K.H., SAKMANN, B., STOCKER, M., GIESE, K.P., PERSCHKE, A., BAUMANN, A. & PONGS, O. (1989). Molecular basis of functional diversity of voltage-gated potassium channels in mammalian brain. *EMBO J.*, **8**, 3235–3244.

WANG, H., KUNKEL, D.D., MARTIN, T.M., SCHWARTZKROIN, P.A. & TEMPEL, B.L. (1993). Heteromultimeric K^+ channels in terminal and juxtaparanodal regions of neurons. *Nature*, **365**, 75–79.

WOOD, J.N., WINTER, J., JAMES, I.F., RANG, H.P., YEATS, J. & BEVAN, S. (1988). Capsaicin-induced ion fluxes in dorsal root ganglion cells in culture. *J. Neurosci.*, **8**, 3208–3220.

(Received February 24, 1994
Revised July 1, 1994
Accepted July 11, 1994)